

## EFFECT OF FLUORINE DOPING CONCENTRATION ON SEMICONDUCTIVE PROPERTY OF TIN DIOXIDE

W. ZHENG\*, Y.N. ZHANG, J.Q. TIAN

*Collage of Material Science & Engineering, Harbin University of Science and Technology, Harbin, 150040, P.R.China*

F-doped SnO<sub>2</sub> (FTO) is one of commercial transparent and conductive oxides with the relatively lower average transmittivity of about 80% in visible region for FTO glass. Decreasing F doping concentration is an efficient way to increase the transmittivity, nevertheless, at the cost of lowering the conductivity of FTO. For determining optimal F doping concentration, semiconductive properties are measured through Hall Effect to discuss the effect of F element amount on charge carrier transportation in FTO. FTO powder morphology and composition were analyzed with FTIR, XRD, SEM and TEM compared with those of the undoped. According to the results, the charge carrier mobility decreases with the increase of F doping concentration, and carrier concentration will increase due to the ionization of F as a donor impurity before the degenerating effect occurs in the situation for heavy doping. The maximum value of carrier concentration,  $1.2 \times 10^{20} \text{ cm}^{-3}$ , can be reached when molar ratio of F/Sn is 3/20, and at this point, the sheet resistance shows the minimum value of  $104 \Omega \text{ sq}^{-1}$  with satisfied average transmittivity of about 90% in visible region.

(Received April 25, 2017; Accepted July 21, 2017)

*Keywords:* F-doped SnO<sub>2</sub>, Hall Effect, carrier mobility, sheet resistance, transmittivity

### 1. Introduction

Doped SnO<sub>2</sub> has been the research emphasis of transparent conducting oxides (TCO) due to its wide band gap, high conductivity and transmittivity [1]. A lot of doping elements, such as Mn [2,3], Ta [4,5], Sb [6, 7], In [8] and F [9,10], have been attempted to improve the electrical conductivity of intrinsic semiconductor SnO<sub>2</sub>. The source of F is extensive and low-cost compared to other elements. Moreover, because the ionic radius of F<sup>-</sup> is similar to that of O<sup>2-</sup> ( $R_{O^{2-}} = 1.32 \text{ \AA}$ ,  $R_{F^-} = 1.33 \text{ \AA}$ ), F is doped more easily without the crystal lattice distortion in SnO<sub>2</sub>. Therefore, the F-doped tin oxide (FTO) has been one of the most common commercial TCO films in industrial production [11].

The FTO films are prepared with several coating techniques, including spray pyrolysis [12], chemical vapor deposition (CVD) [13] and sol-gel method [14]. Wu et al [15] have fabricated the powder slice of F-doped tin dioxide by sol-gel method and got the surface resistance of  $110 \Omega \text{ sq}^{-1}$ . Chinnappaa et al [16] reported that FTO films were deposited using a simplified spray technique and suggested that the minimum sheet resistance is  $42.59 \Omega \text{ sq}^{-1}$ . However, they mainly reported the electrical properties of FTO films and did not analyze the influence of F concentration on optical performance [17]. Transmittivity of both the reported and commercial FTO glass are about 80%. As we know, trace amount doping would change the photoelectrical property of semiconductor significantly. According to solid state physics theory, the transmittivity will be increased with decreasing F concentration in FTO, and therefore we try to lower F doping concentration to enhance the transparency at least cost for electrical conductivity of FTO. In this work, carrier transporting process is discussed in Hall Effect measurement with various F doping concentration FTO glass, through which a suitable F concentration in semiconductive tin oxide can be determined considering both transparency and conductivity of FTO.

---

\*Corresponding author: zhengwei1972@sina.com

## 2. Preparation of FTO Samples

F-doped SnO<sub>2</sub> nanocrystals were synthesized with a combinative sol-gel hydrothermal method. In a typical procedure, 11.3 g SnCl<sub>2</sub>•2H<sub>2</sub>O was dissolved in 5 ml concentrated hydrochloric acid under magnetic stirring and pH value of 7 can be reached through adding aqueous ammonia drop by drop. The mixture solution was heated in water-bath at 80°C for 5 h and the obtained precipitation was filtered and washed with deionized water to remove impurity ions. And then moderate hydrofluoric acid was added into the precipitation in different molar ratio of F/Sn (1/20, 2/20, 3/20, 4/20, 10/20, 20/20, 40/20). After stirring the solution, hydrothermal process was carried out at 200°C for 12 h in an 80 ml autoclave. Finally, the washed and dried powder was sintered at the optimal sintering temperature, and the treated powder was pressed into thin slice (Φ10×4 mm) for property characterization. The FTO thin film was coated through spin-coating on the transparent glasses (10×20×2 mm).

## 3. The Characterization of FTO powder

Differential thermal analysis (DTA) and thermo-gravimetric analysis (TG) are carried out to research the conversion process of the F-doped SnO<sub>2</sub> powder during calcination for confirming appropriate sintering temperature eventually. Fig.1 shows the change of weight percentage and temperature difference with the elevated temperature (from 20 to 600°C). TG curve exhibits that sample weight percentage keeps stable without obvious change before 300°C and then changes due to a slight endothermic phenomenon occurs in this temperature range according to the DTA curve. It can be explained that Sn<sup>2+</sup> has been transformed to SnO during hydrothermal reaction in experimental process.

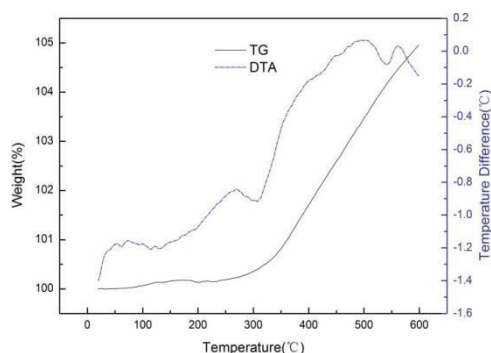


Fig.1. DTA-TG curves of the FTO powder sample (F/Sn= 3/20, prepared hydrothermally at 200 °C for 12h)

SnO is stable under 300°C, while the existence of temperature difference is the result of dehydration. The weight of sample increases obviously between 300°C and 600°C, an exothermic peak at 500°C and another characteristic endothermic peak followed at 530°C during the whole endothermic process. The two peaks are attributed to the generation of SnOF and SnO<sub>2</sub> from SnO between 300°C and 450°C, respectively [15], which means F can be doped in this temperature range. With the rise of temperature continually, F deprivation from SnOF to SnO<sub>2</sub> will occur, which results in exothermic peak and obvious endothermic tendency. Thus, we define the appropriate temperature of sintering is 450°C in the following work.

Fourier transform infrared spectroscopy (FTIR) of the undoped powder sample (a) and F-doped sample (b) are measured to identify the location of doped F ions in Fig. 2. According to standard spectrum, the absorption peaks between 400 cm<sup>-1</sup> and 700 cm<sup>-1</sup> are attributed to the

vibrations of Sn-O and Sn-O-Sn in  $\text{SnO}_3^{2-}$  atom group. Compared to undoped sample, there is an obvious splitting peak around  $594\text{ cm}^{-1}$  in spectrum of F-doped sample, which illustrates that F atom has been doped successfully. Because  $\text{F}^-$  exhibits a higher electro-negativity than  $\text{O}^{2-}$ , F doping would result in the higher vibration energy of chemical bond, which will make the absorption peaks move to the left, a higher wavenumber and lead to the splitting phenomenon in Fig.2 (b). The peak between  $1600\text{ cm}^{-1}$  and  $1700\text{ cm}^{-1}$  is attributed to the vibration of Sn-OH [15, 18], which indicates partial Sn-OH has not participated in the reaction in preparation process.

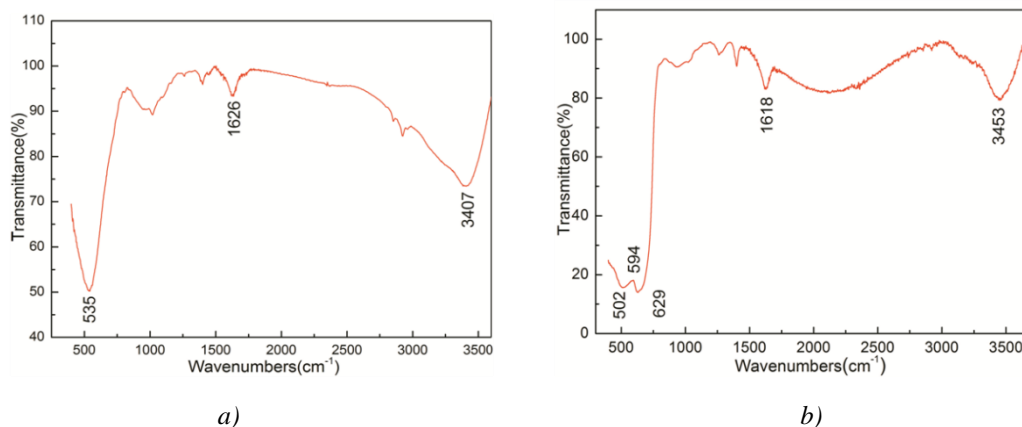


Fig. 2. FT-IR spectra of the undoped (a) and the F-doped ( $\text{F}/\text{Sn} = 3/20$ ) $\text{SnO}_2$  powder samples (b) sintered at  $450\text{ }^\circ\text{C}$  for 30 min

The crystal structure of prepared undoped and F-doped powder samples were characterized by X-ray diffraction (XRD) in Fig.3. All characteristic diffraction peaks are well-matched with standard peaks of tetragonal rutile  $\text{SnO}_2$  crystal according to the reference pattern (JCPDS 880287) [19]. Compared with undoped sample, the relative intensity of lattice plane (101), (200) and (211) to lattice plane (110) are changed from 69.7%, 20% and 46.7% to 72.69%, 23.5% and 51.7% after doping F treatment, respectively. The slight change of relative intensity demonstrates that F has been doped into  $\text{SnO}_2$  crystal assuredly and just locates the site in crystal lattice. The locations of these peaks have not been shifted, which means the tetragonal crystal structure has not changed because of the similar atomic radius between F (0.133nm) and O (0.132nm). Meanwhile, the crystalline size of prepared  $\text{SnO}_2$  nanocrystal is about 20 nm calculated by Scherrer's Equation [20, 21]. Fig.4 shows the scanning electron microscope (SEM) and transmission electron microscopy (TEM) images of the pure  $\text{SnO}_2$  powder (a) and F-doped  $\text{SnO}_2$  (b). Spherical particles generated after sintering and the average grain size is about 20 -30nm from the TEM images, which is consistent with the result obtained from XRD analysis.

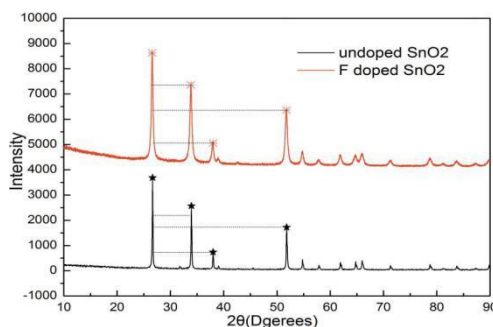


Fig. 3. XRD patterns of the undoped and F-doped ( $\text{F}/\text{Sn} = 3/20$ ) $\text{SnO}_2$  powder samples sintered at  $450\text{ }^\circ\text{C}$  for 30 min

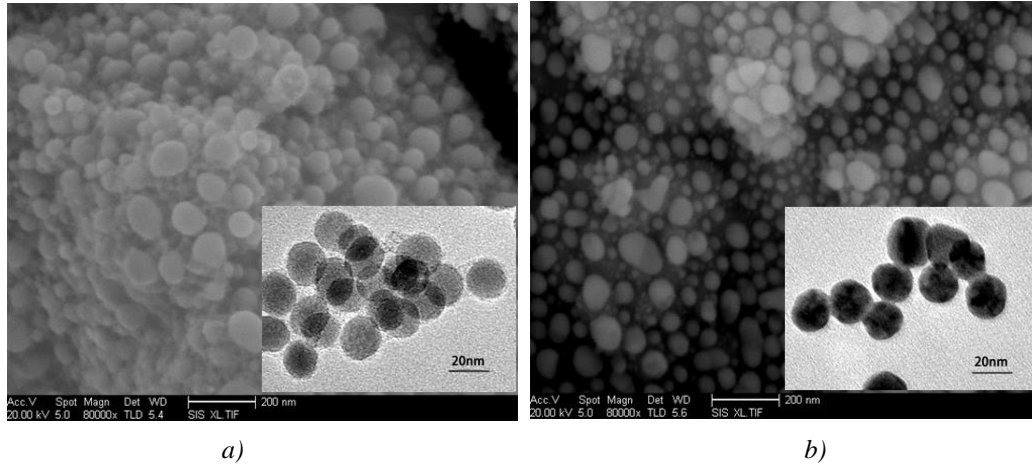


Fig. 4. SEM and TEM photos (lower right corner) of the undoped (a) and F-doped ( $F/Sn=3/20$ )  $SnO_2$  powder samples (b) sintered at 450 °C for 30 min

#### 4. The Performance of FTO films

FTO glass samples with different F/Sn molar ratios were characterized with Hall Effect measurement system to analyze the effect of F content on  $SnO_2$  semiconductive property. Fig.5 illustrates the changes of carrier concentration (CC), mobility and sheet resistance (SR) with different F/Sn molar ratio. With the increase of the F-doped concentration, the carrier concentration exhibits a trend of decrease after the first increase from the black curve in Fig.5. Usually, the concentration of ionized donor can be calculated theoretically with the following equation in intrinsic element semiconductor:

$$n_d^+ = \frac{N_D}{1 + 2 \exp[(E_F - E_D)/KT]} \quad (1)$$

Where  $N_D$  is the concentration of donor impurity,  $E_F$  is the Fermi level,  $E_D$  is conduction band energy,  $T$  is temperature and  $K$  is Boltzmann constant. According to Equation (1), carrier concentration should increase significantly and then slightly with increase of donor doping concentration because of degenerating effect ( $E_F = E_D$ ). But for intrinsic compound semiconductor, the situation is more complicated. When the F doping concentration is low, the concentration of carriers derived from the F atom as donor impurity rises in non-degenerative n-type semiconductor, FTO. At this time, the donor impurity is completely ionized. But, when F doping concentration is higher, Fermi level will approach the conduction band or even overlap it, i. e. the degenerating effect follows. In this case of degenerative FTO, the carrier concentration decreases because only part of the doped donor is ionized and the other is not [22]. Moreover,  $SnOF$  will change to  $SnOF_2$ , which was indicated in Fig. 1 and F ions won't be donors anymore. Thus, carrier concentration shows a declining trend with the increase of F doping. The mobility shows a trend of continuous declining with the increase of F doping concentration from the red curve in Fig.5. Normally, mobility is affected by scattering including acoustic wave scattering and ionized impurity scattering for doped semiconductor, the total mobility is:

$$\varphi = \frac{q}{m^*} = \frac{1}{AT^{3/2} + B \frac{Ni}{T^{3/2}}} \quad (2)$$

Where  $q$  is unit charge,  $m^*$  is effective mass,  $Ni$  is concentration of ionized impurity,  $T$  is temperature,  $A$  and  $B$  are constants. Since the lattice vibration energy doesn't change at room temperature, acoustic wave scattering can be ignored. While the concentration of impurity plays a

key role in ionized impurity scattering, and combining with the equation (2), the higher impurity concentration will lead to the stronger ionized impurity scattering and the smaller mobility [23]. Thus, carrier mobility declines with the increase of doping concentration.

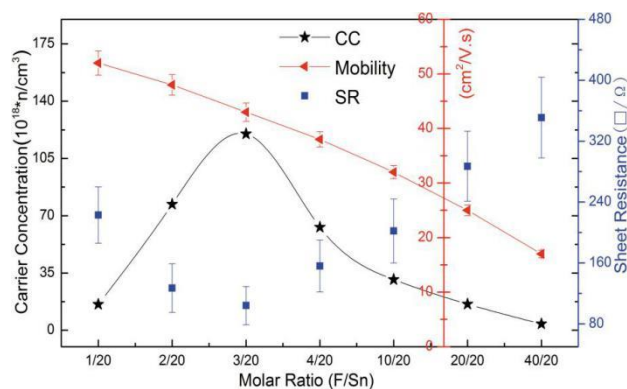


Fig. 5. Hall measurement curves of the F-doped  $SnO_2$  samples with different F/Sn molar ratios

With the increase of the F doping concentration, the sheet resistance decreases and then increases from the SR curve in Fig.5. The sheet resistance was determined by two factors: carrier concentration and mobility. When F doping concentration is low, the sheet resistance reduces with the increase of doping proportion owing to the increase of carrier concentration [24]. At this time, the mobility reduces slightly, so it can be offset. When F doping concentration exceeds a certain value, the sheet resistance increases obviously, which contributes to the incomplete ionization of F impurity in semiconductor under heavy doping and the decrease of mobility [25].

Fig. 6 shows the transmittance curves of FTO samples with different F concentrations in the wavelength range 300-1000nm. The average transmittivity is 90.2% for the sample (F/Sn=3/20), and it decreases with the further increase of F-doping content in accordance in Lambert-Beer Law. The average transmittivity (90%) is absolutely higher than that of some commercial FTO glass (usually 80%, in visible region of 300-800 nm). The color of the slight doping film is colorless and the higher F concentrations result in a dark green film. Tab.1 lists the result of transmittivity and the sheet resistance measured with four-point probe method for different samples. As can be seen from Table 1, the sheet resistance shows the minimum value when molar ratio of F/Sn is 3/20. And at this point, the sheet resistance shows the minimum value of  $104 \Omega \text{ sq}^{-1}$  with satisfied average transmittivity of about 90% in visible region. And the transmittivity decreases gradually with the increase of fluorine doping concentration. The carrier concentration increases in the beginning, and then becomes lower with the increase of fluorine doping concentration. Also the carrier traps increase and carrier mobility decreases with the increase of fluorine doping concentration. So the resistance shows the minimum value when molar ratio of F/Sn is 3/20.

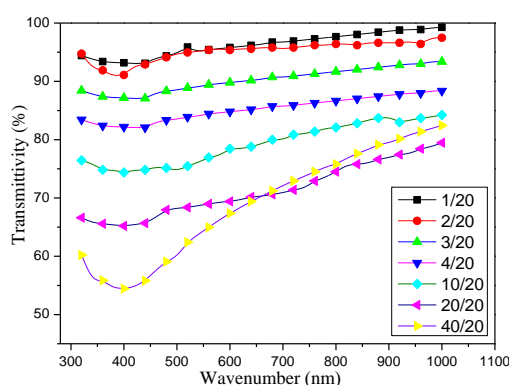


Fig.6. Transmission spectra of FTO samples with different different F/Sn molar ratios

Table.1 The transmittivity and sheet resistance of FTO samples with different F/Sn molar ratio

Sample(F/Sn ratio)	1/20	2/20	3/20	4/20	10/20	20/20	40/20
Transmittivity(%)	96%	95%	90%	85%	79%	71%	68%
sheet resistance ( $\Omega\text{sq}^{-1}$ )	231	128	104	159	202	285	355

## 5. Conclusions

F-doped  $\text{SnO}_2$  nanocrystals have been fabricated successfully by sol-gel hydrothermal method. The appropriate sintering temperature of is  $450^\circ\text{C}$  according to the TG-DTA curves. The results of XRD and FT-IR test prove the F has been doped into the  $\text{SnO}_2$  crystal assuredly. F Doping can effectively improve the carrier concentration and reduce the sheet resistance of  $\text{SnO}_2$  semi-conductor from Hall measurement. But, heavy doping is disadvantageous to both carrier concentration and the conductivity of semi-conductor. When the molar ratio of F/Sn is 3/20, transmittivity of the sample is about 90% in the range of 300-1000 nm and the sheet resistance can reach the minimum  $104 \Omega \text{sq}^{-1}$ . At this point, the carrier concentration and mobility are  $1.2 \times 10^{20} \text{cm}^{-3}$  and  $42 \text{cm}^2 / \text{V}\cdot\text{s}$ , respectively.

## Acknowledgement

This work was supported by Program for New Century Excellent Talents in Heilongjiang Provincial University (1155-NCET-009), Science and Technology Innovation Talents of Harbin (2013RFXXJ004) and the Scientific Research Foundation for the Returned Overseas Chinese Scholars of State Education Ministry(SRF for ROCS, SEM2011).

## References

- [1] E. K. Liu, B. S. Zhu, J. S. Luo, The Physics of Semiconductors, seventh edition, Electronic Industry Press, Beijing, 2011.
- [2] Y. H. Xiao, S. H. Ge, L. Xi, Y. L. Zuo, X. Y. Zhou, B. M. Zhang, L. Zhang, C. X. Li, X. F. Han, Z. C. Wen, *Appl. Surf. Sci.* **254**, 7459 (2008).
- [3] K. Anandan, V. Rajendran, *Superlattice Microstruct.* **85**, 185 (2015).
- [4] G. Turgut, *Thin Solid Films* **594**, 56 (2015).
- [5] S. Nakao, N. Yamada, T. Hitosugi, Y. Hirose, T. Shimada, T. Hasegawa, *Thin Solid Films* **518**, 3093 (2010).
- [6] S. H. Yu, W.F. Zhang, L. X. Li, D. Xu, H. L. Dong, Y.X. Jin, *Appl. Surf. Sci.* **286**, 417 (2013).
- [7] W.H. Yang, S.H. Yu, Y. Zhang, W.F. Zhang, *Thin Solid Films* **542**, 285 (2013).
- [8] D.M. Xu, K. Pan, X.W. Liu, X.J. Wang, W.Z. Wang, C.J. Liang, Z. Wang, *Chinese Journal of Catalysis* **37**, 2018 (2016).
- [9] B. J. Li, L. J. Huang, N.F. Ren, X. Kong, Y. L. Cai, J.L. Zhang, *Appl. Surf. Sci.* **351**, 113 (2015).
- [10] A.H.O. Alkhayatt, S. K. Hussian, *Mater. Lett.* **155**, 109 (2015).
- [11] Q. Gao, Q.Y. Liu, M. Li, X. Li, Y. Liu, C.L. Song, J.X. Wang, J.B. Liu, G. Shen, G.R. Han, *Thin Solid Films* **544**, 357 (2013).
- [12] L. Chinnappaa, K. Ravichandran, K. Saravanakumarb, N. Jabenabegumc, B. Sakthivel, *Surf. Eng.* **27**, 770 (2011).
- [13] N. Noor, I.P. Parkin, *J. Mater. Chem.* **1**, 984 (2013).
- [14] Q.P. Tran, J.S. Fang, T.S. Chin, *Mater. Sci. Semicond. Process.* **40**, 664 (2015).
- [15] S.S. Wu, S. Yuan, L.Y. Shi, Y. Zhao, J. H. Fang, *J. Colloid Interface Sci.* **346**, 12 (2010).
- [16] Y. Wang, K.W. Xu, *Acta Phys. Sin.* **53**, 900 (2004).
- [17] X.H. Shi, K.J. Xu, *J. Materials. Science In Sem. Pro.* **58**, 1 (2017).
- [18] V. Senthilkumar, P. Vickraman, R. Ravikumar, *J. J Sol-Gel Sci Technol.* **53**, 316 (2010).
- [19] A. N. Banerjee, S. Kundoo, P. Saha, K. K. Chattopadhyay, *J. J Sol-Gel Sci Technol.* **28**, 105 (2003).
- [20] K. Ravichndran, G. Muruganatham, B. Sakthivel, *J. Physical B.* **404**, 4299 (2009).
- [21] Z. Lou, L. Wang, R. Wang, Z. Tong, *J. Solid-State Electronics.* **76**, 91 (2012).
- [22] G. C. Xi, Y.T. He, Q. Zhang, H.Q. Xiao, X. Wang, C. Wang, *J. The Journal of Chemical Physics.* **112**, 11645 (2008).
- [23] A.G. Chitra, S.S Major, *J. J Mater Sci*, **31**, 2965 (1996).
- [24] A.V. Moholkar, S.M. Pawar, K.Y. Rajpure, C.H. Bhosale, *J. Alloys Compd.* **455**, 440 (2008).
- [25] B. Russo, G.Z. Cao, *J. Applied Physics A.* **90**, 311 (2008).